Title

Antidiabetic “gliptins” affect biofilm formation by *Streptococcus mutans*

Authors

Arpan De[a], Arianna Pompilio[b,c], Jenifer Francis[d], Iain C. Sutcliffe[d], Gary W. Black[d], Giulio Lupidi[a], Dezemona Petrelli[e], Luca A. Vitali[a]*

Authors’ affiliation

a. School of Pharmacy, University of Camerino, 62032, Camerino, Italy.
b. Department of Medical, Oral and Biotechnological Sciences, School of Medicine, "G. d'Annunzio" University of Chieti-Pescara, 66100, Chieti, Italy.
c. Center of Excellence on Ageing, "G. d'Annunzio" University Foundation, 66100, Chieti, Italy.
d. Department of Applied Sciences, Faculty of Health & Life Sciences, Northumbria University, NE1 8ST, Newcastle upon Tyne, UK
e. School of Biosciences and Veterinary Medicine, University of Camerino, 62032, Camerino, Italy.

Corresponding Author

Vitali Luca Agostino
ph. +39-0737-403282, fax +39-0737-403281, Email: luca.vitali@unicam.it

Abstract

Streptococcus mutans, a dental caries causing odontopathogen, produces X-prolyl dipeptidyl peptidase (Sm-XPDAP, encoded by *pepX*), a serine protease known to have a nutritional role. Considering the potential of proteases as therapeutic targets in pathogens, this study was primarily aimed at investigating the role of Sm-XPDAP in contributing to virulence-related traits. Dipeptidyl peptidase (DPP IV), an XPDAP analogous enzyme found in mammalian tissues,is a well known therapeutic target in Type II diabetes. Based on the hypothesis that gliptins, commonly used as anti-human-DPP IV drugs, may affect bacterial growth upon inhibition of Sm-XPDAP, we have determined their *ex vivo* antimicrobial and anti-biofilm activity towards *S. mutans*. All three DPP IV drugs tested reduced biofilm formation as determined by crystal violet staining. To link the observed biofilm inhibition to the human-DPP IV analogue present in *S. mutans* UA159, a *pepX* isogenic mutant was generated. In addition to reduced biofilm formation, CLSM studies of the biofilm formed by the *pepX* isogenic mutant showed these were comparable to those formed in the presence of saxagliptin, suggesting a probable role of this enzyme in biofilm formation by *S. mutans* UA159. The effects of both *pepX* deletion and DPP IV drugs on the proteome were studied using LC-MS/MS. Overall, this study highlights the potential of Sm-XPDAP as a novel anti-biofilm target and suggests a template molecule to synthesize lead compounds effective against this enzyme.

Keywords

Streptococcus mutans; Biofilm, X-prolyl dipeptidyl peptidase; saxagliptin; shot-gun proteomics

Introduction

Dental caries is the most prevalent, multifactorial, globally increasing oral health problem among children and adults (Bagramian et al., 2009; Selwitz et al., 2007). It is a manifestation of biofilm formation by certain members of the indigenous oral microbiota that are aciduric and acidogenic. Among them, *Streptococcus mutans* is one of the key etiological agents of dental caries. *S. mutans* is known to code for several peptidases and exoglycosidases that can facilitate utilization of human saliva as a source of nutrition (Ajdić et al., 2002). X-prolyl dipeptidyl aminopeptidase (XPDAP) is one such narrow substrate range cytoplasmic endopeptidase found in *S. mutans*, which help in utilization of proline-rich salivary polypeptides (Cowman and Baron, 1997, 1993). Collagenolytic and caseinolytic activities demonstrated by XPDAP further suggest its importance as a putative virulence factor in *S. mutans* (Cowman *et al.*, 1975; Rosengren & Winblad, 1976). In *Streptococcus suis* and *Streptococcus gordonii* extracellularly present XPDAP play a role also in cellular invasion (Ge et al., 2009; Goldstein et al., 2001). Similarly, periodontal pathogen *Porphyromonas gingivalis* also had altered virulence in absence of XPDAP (Yagishita et al., 2001).

An analogous enzyme to XPDAP, DPP IV is also found in mammalian tissues and is a target for maintaining glucose homeostasis in Type II diabetic patients (Cowman and Baron, 1997; Green et al., 2006). Diabetes, an abnormal metabolic disorder, is an epidemic of significant healthcare concern among both developed and developing countries (King et al., 1998). Certain drugs, namely saxagliptin, vildagliptin and sitagliptin, are commonly used anti-human DPP IV (AHD) molecules used in the treatment of Type II diabetes (Green et al., 2006). DPP IV targets incretin hormones such as GLP-1, thereby decreasing their plasma levels. Inhibition of DPP IV leads to

64 the opposite effect, which results in a restoration of glucose homeostasis in diabetic patients
65 (Wang et al., 2012). As a novel approach, our recent investigation has shown that *S. mutans*
66 XPDAP (Sm-XPDAP, encoded by *pepX*) is inhibited by saxagliptin *in vitro* (De et al., 2016). In
67 an extension of this work and hypothesising a probable role of Sm-XPDAP in virulence, herein
68 we have evaluated the *ex vivo* effect of these molecules on cell growth and biofilm formation by
69 *S. mutans*. A *pepX* (SMU.35) isogenic mutant was also generated. Furthermore, whole cell
70 proteome analysis of AHD treated cells and the isogenic mutant was performed to identify
71 possible consequences of Sm-XPDAP inhibition or deletion.

72 **Materials and Methods**

73 *MIC and Biofilm formation assay*

74 The MIC was determined by microdilution assay according to the Clinical and Laboratory
75 Standards Institute (CLSI, 2011), with the exception of the medium used, which was BHI (Ahn
76 et al., 2012; da Silva et al., 2013). The highest concentration of 2048µg/mL of each AHD was
77 serially diluted down to 4µg/mL and the final density of mid-exponential phase cells used was
78 10^6 CFU/mL. The drugs were dissolved in sterile water and erythromycin was used as a positive
79 control.

80 Biofilm formation was assessed by a semi-quantitative crystal violet method in polystyrene 96-
81 well cell culture plates (Costar 3595; Corning Inc., NY) as previously described (Ahn et al.,
82 2008). An overnight culture of *S. mutans* UA159 (ATCC 700610) was transferred into pre-
83 warmed BHI and grown till mid-exponential phase and then diluted 50 fold in semi-defined
84 biofilm medium (SDM) supplemented with 20mM glucose or sucrose. Aliquots (100µL) of this
85 culture were added to serially diluted drug in water (2048µg/mL to 4µg/mL), to make a final

86 volume of 200µL (with a 100-fold final dilution of cells) and incubated for 20 hours. The
87 adhered cells were stained with 1% crystal violet for 15 minutes and the extract was quantified at
88 495nm. The viability of the cells in the culture medium (planktonic phase over the formed
89 biofilm) at each concentration of drug was determined by CFU counting.

90 *Construction of pepX deletion mutants*

91 A *pepX* deletion mutant was generated by PCR ligation mutagenesis method (Lau et al., 2002).
92 Briefly, erythromycin cassette, upstream and downstream flanking regions (about 600bps) of
93 *pepX* was amplified using specific primers (Table 2). The amplicons were digested using NcoI
94 and SacI and ligated at 16^{o}C overnight. The resulting ligation mixes were used for PCR to obtain
95 a mutagenic construct using primers pepX-Up-F and pepX-Dn-R. This fragment was naturally
96 transformed into mid-log phase *S.mutans* UA159, grown in Todd-Hewitt broth containing 10%
97 sucrose and the recombinants were selected on BHI agar containing 10µg/mL erythromycin
98 (Petersen and Scheie, 2000).*The pepX* mutant was confirmed by colony PCR and Sanger
99 sequencing.

100 *CLSM examination of Biofilm*

101 The structure of biofilm of the *pepX* mutant and wild-type *S. mutans*, grown on polystyrene discs
102 in the presence of SDM and glucose and AHD drugs as described above, was evaluated using an
103 LSM-510-META laser scanning microscope attached to an Axioplan-II microscope (Zeiss). The
104 non-adherent cells were washed in saline, biofilms were stained with Live/Dead BacLight-(1X)
105 (Molecular Probes Inc.) for 20 minutes and rinsed three times in saline to remove excess stain.
106 Subsequently, the stained discs were examined with an alpha Pan-Fluor 100X objective under
107 excitation at 488nm (Argon-laser) and 543nm (He-Ne-laser), and emission filter ranging 585-

615nm and 505-530nm for Propidium iodide and SYTO9, respectively. ImageJ v1.48 (NIH, USA) was used to process images. The proportion of viable cells (green) versus dead cells (red) was determined based on the intensity at each pixel using ImageJ (Nance et al., 2013). The proportion of green signal and the red signal was calculated by multiplying the total number of pixels with the given intensity (0 -255) at each channel and then dividing it by the sum of the intensity value for each signal measured at each image stack.

Proteome analysis of biofilm-grown cells

The proteome of biofilm-grown cells in absence or presence of an AHD drug and that of the Δ*pepX* mutant were analysed from 48mL of culture. In brief, after 20 hours incubation, the harvested biofilm cells were lysed. The lysate was used to acetone precipitate all proteins overnight at -20°C. The precipitate was washed in 80% and 40% acetone successively, air dried and then partially pre-fractionated by 1D PAGE. The protein containing gel was stained, destained and sectioned into pieces for treatment in 100mM NH_4HCO_3 and acetonitrile (ACN) for complete removal of Coomassie stain. The gel slices were dehydrated in ACN and digested in 40µg/mL trypsin (Trypsin Gold, MS Grade, Promega) at 37°C overnight. Digestion was then stopped by adding 50% ACN (v/v) and 5% formic acid (v/v) with shaking for 30 min. The peptides-containing digested extract was removed and the gel pieces were further extracted in ACN and formic acid before freeze drying. The lyophilized peptide digest was mixed in 5% ACN and 0.1% formic acid (v/v) and then run in a LC-NanoPump coupled to a tandem mass spectrometer (Thermo-Q-Exactive attached to HPLC Ultimate-3000-RSLCnano system), through an Easy Spray C18 column (PepMap-RSLC, 75µm×500mm, Thermo Scientific) in a gradient solvent mixture of water and ACN containing 0.1% formic acid. The run was carried out for 215 minutes at a flow rate of 0.3µL/min with a scan range of 350–1800 m/z. The mass

spectrum data (MS and MS^2) was then processed in Progenesis LC-MS v4.1 and the peptides identified in MASCOT database (Matrix Science, UK).

Statistical analysis

Statistical analysis was performed using the software Statgraphics Centurion ver. XV (Statpoint Technologies, Inc., Virginia, USA). Fitting of data was done using Origin ver. 8.1 (Origin Lab Corporation, MA, USA). Inhibition of biofilm formation data were fitted using a dose/response function (Boltzmann), according to the following equation (1):

$$y = A2 + \frac{A1 - A2}{1 + e^{(x - EC50)/dx}} \qquad (1)$$

where A2 and A1 are the maximum and minimum level of biofilm formed, respectively, and EC_{50} is the concentration of the drug affecting 50% biofilm formation. EC_{50} values from the four replicates of the same drug were derived and their mean calculated. Distribution of EC_{50} values of the same drug was checked for normality. Analysis of variance (ANOVA) test was run to compare means from different drugs and to check variance. Probability value threshold was set to 0.05. Multiple comparison analysis was performed between pairs of data sets (considered as independent), corresponding to biofilm formation level (OD_{490nm}) at each and every concentration of the given drug. F-test (ANOVA) was used to test for the rejection of the null hypothesis ($P < 0.05$).

Results

AHD drugs inhibited biofilm formation by S. mutans

AHD drugs did not show a visible growth inhibition effect in the concentration range studied (4–2048 μg/mL). In the presence of sucrose, *S. mutans* sessile growth was not affected by any of the drugs, whereas all three AHD drugs inhibited biofilm formation in the presence of glucose, albeit with different potency (Fig. 1A). At concentrations >128 μg/mL of saxagliptin, there was 50% reduction of biofilm formation. Vildagliptin inhibited biofilm formation at concentrations ≥ 256μg/mL, while sitagliptin demonstrated at least 50% inhibition at 256μg/mL, albeit with a substantial increase in biofilm biomass at 2048μg/mL. The EC_{50} values of all drugs fell within the range of 128-512μg/mL. However, in the case of sitagliptin, the data point at 2048 μg/mL was not considered for fitting due to the anomalous behaviour at that concentration. While saxagliptin exhibited a more consistent inhibition pattern at concentrations ≥ 64 μg/mL, sitagliptin gave a sudden drop till saturation at 256-1024 μg/mL (Supplementary Fig.S1), as confirmed by the lower EC_{50} value (Table 1). In the case of saxagliptin and sitagliptin, the F-test (ANOVA) showed a statistically significant difference between the means at each concentration ($p_{saxagliptin} = 0.0013$, $p_{sitagliptin} = 0.0089$).To determine which means are significantly different from which other and to analyse the difference in effect at various concentrations, a multiple sample pairwise comparison of the means of the four independent measurements of biofilm formation at each drug concentration (number of concentrations n = 11, from 0 to 2,048μg/mL) was performed (Supplementary Fig. S2). The apparent increase in biofilm formation at 2048μg/mL of sitagliptin was found to be statistically relevant when compared with the biofilm biomass formed in presence of 128, 256, 512, and 1024 μg/mL of the drug (Supplementary Fig. S2b, cyan points). The differences observed in the presence of vildagliptin were not significant.

The cells in the planktonic phase over the formed biofilm at each concentration of drug were equally viable with colony count at 64µg/mL-2048µg/mL of each AHD treatment ranging between 10^9 to 10^{10} CFU/mL (Supplementary Fig. S3).The control group ($8.23\pm1.7\times10^8$CFU/mL) differed by one order of magnitude from the colony counts at 2048µg/mL of each drug ($p = 0.043$, unpaired student t-test, two-tailed).

pepX mutant exhibited reduced biofilm biomass

The stronger effect of saxagliptin on biofilm compared to the other two AHD drugs, concomitant with a lower K_i of this drug against pure recombinant enzyme (De et al., 2016), suggested a probable role of *pepX* in influencing biofilm formation by *S. mutans*. To confirm a direct involvement of Sm-XPDAP in the biofilm development, a *pepX* mutant was generated. Crude extracts from the deletion mutant showed no amidolytic activity. The growth rate of the *pepX* deletion mutant was comparable to that of the wild type both in BHI (data not shown) and inSDM (Supplementary Fig. S4, $P = 0.317$ by ANOVA for the variable "growth rate"), however, the CFU of mutant significantly differed from that of the wild type hinting towards less viability of *pepX* mutant in SDM (Supplementary Fig. S4, $P < 0.01$ by ANOVA for the variable "growth rate"). The biofilm of the Δ*pepX* mutant in SDM containing glucose was reduced by 70% (SD = 13.4%, n = 9, Fig. 1B), while a lower decrease was observed in presence of sucrose (20%; SD = 3.8%, n = 3, data not shown).The planktonic phase over the biofilm of *pepX* mutant had more viable cells compared to wild type (Fig 1B, insert), which may indicate that the mutant cells aggregate or adhere to the surface of the well less efficiently with a high propensity to remain in suspension. The same was for biofilms formed in the presence of AHD (Supplementary Fig. S3).

196 *Sm-XPDAP deficiency and saxagliptin treatment induced stress in S. mutans*

197 The adherence of wild-type *S. mutans* treated with saxagliptin or vildagliptin and that of the
198 Δ*pepX* mutant determined at 4h did not show any difference when compared to the untreated
199 wild-type. At 20h, the wild-type demonstrated a thick and dense homogenous layer of
200 aggregated cells, apparently more viable with few void spaces (15µm and 70.4% green cells,
201 respectively), whereas the Δ*pepX* mutant exhibited a less organized thin layer of cells with more
202 void spaces (9.6µm and 28.5% green cells) (Fig. 2). The effect of saxagliptin on wild-type was
203 similar to that of Δ*pepX*. At 512 µg/mL saxagliptin, streptococci showed shorter dispersed chains
204 and experienced apparent stress with a higher prevalence of propidium iodide stained cells (36%)
205 (Fig. 3e and 3f). Vildagliptin also led to disaggregation of the biofilm compared to the untreated
206 control, but streptococcal chains looked healthier (Fig.3g). *S. mutans* grown in the presence of
207 2048µg/mL sitagliptin presented a biomass level comparable to the untreated cells. However,
208 chains were relatively long, apparently under stress with no difference in aggregation and in the
209 proportion of dead cells (Fig. 3h and 3i).

210

211 *pepX mutant exhibited downregulation of Cell Surface Antigen I/II*

212 The proteomic analysis for differentially expressed proteins confirmed the absence of PepX in
213 the Δ*pepX* mutant. Using relatively stringent criteria for protein identification (>1 peptide
214 identified per protein in each biological replicate) only 9 proteins were found to be more
215 abundant in the wild-type compared to the Δ*pepX* mutant (Supplementary Table S1) and no
216 proteins were more abundant in the mutant compared to wild-type. Notably, the differentially
217 expressed proteins included the Cell Surface Antigen I/II, a well-characterised adhesion protein

of *S. mutans* (Jenkinson and Demuth, 1997). Notably, three of these 9 proteins were amino acid tRNA ligases. Comparison of control and sitagliptin-treated biofilms identified 6 proteins as more abundant in the controls and 26 as more abundant in the drug-treated cells. Likewise, comparison of control and saxagliptin-treated biofilms identified 6 proteins as more abundant in the controls (including three glycosyltransferases and levansucrase, which may affect biofilm matrix formation) and 23 as more abundant in the drug-treated cells. Two of the glycosyltransferases (SMU.910 and SMU.1005), upregulated in the controls compared to saxagliptin-treated biofilms, were upregulated in the sitagliptin-treated biofilms suggesting drug specific responses that may affect biofilm remodelling. Of 49proteins differentially expressed in either drug treatment, 12 were noted to be consistently altered in both (Supplementary Table S1) and were primarily involved in protein synthesis (n = 4) and various metabolic pathways (n = 7).

Discussion

The AHD drugs used in this study are highly selective human DPP IV inhibitors (Wang et al., 2012). We hypothesize their effects on *S. mutans* by acting on Sm-XPDAP and regulating the behaviour of the bacterium, even though the drugs may have multiple enzyme targets. The *ex vivo* assays using these gliptins showed inhibition of *S. mutans* biofilm formation. It could be speculated that this may impair streptococcal activity in the oral cavity of diabetic patients on these medications, as a consequence of the excretion of these drugs in saliva. Saxagliptin and vildagliptin have been found to possess 50% and >90% oral bioavailability, respectively (Boulton et al., 2013; Villhauer et al., 2003), while saxagliptin has also been reported in the salivary gland tissue (Fred, 2009). Sitagliptin, which is quite effective against biofilm formation and classified as a high intestinal permeability and low protein binding drug, has been found in saliva (AUC 592 ng/mL×hr) (Idkaidek and Arafat, 2012). This may suggest the possibility of excretion of the other two AHD drugs in saliva, which in conjunction with our results may suggest that systemic basal level of these drugs in host tissue of prescribed users may help in interfering with *S. mutans* behaviour.

In view of the differential cell physiology in sessile form compared to planktonic phase, the very high MIC of AHD drugs was considered inconsequential. CLSM was performed to investigate the influence of AHD drugs and the effect of Sm-XPDAP deficiency on the structural organization of *S. mutans* biofilms *in vitro*. We tested saxagliptin and vildagliptin, the first for its gradual relative effect at each concentration and the second for its consideration as a reference molecule for comparison between “cyanopyrrolidides”. CLSM was conducted at 128 µg/mL saxagliptin and 512 µg/mL vildagliptin, which were the concentrations causing >40% biofilm inhibition (Fig. 1A). Blurred green cells observed under CLSM in biofilm treated with AHD was

indicative of the stress experienced by *S. mutans* in the given condition (Boulos et al., 1999). Cells treated with 512 µg/mL saxagliptin displayed similar observation to that of *pepX* mutant, which may allow hypothesizing that the inhibition of biofilm in presence of AHD drugs may be exerted through Sm-XPDAP inhibition. In contrast to the other AHD drugs, a sudden increase in attached biofilm observed in presence of 2048µg/mL sitagliptin can likely be best explained due to increased stress response. Interestingly, there was complete inhibition of growth at the subsequent higher concentration of sitagliptin (Supplementary Fig. S5). A similar differential response to varying concentrations of the antibiotic lincomycin has also been reported in *Streptococcus pyogenes* (Malke et al., 1981), albeit the mechanism of action has not been explained yet. As a proof of concept, in this study we have used experimental systems as simplified as possible, considering that changes in variables may mask inhibition effects by the tested drugs. Once the fine mechanism of gliptin action in *S. mutans* is unravelled it will be of great interest to investigate how variations in the experimental approach that better emulate the *in vivo* conditions, such as using hydroxylapaptite discs, adding saliva or using a mixed species biofilm model could alter the drug activity.

In this study a preliminary attempt was also made to identify a plausible role of PepX in modulating the proteome and investigate the site of action of AHD drugs in *S. mutans* through whole cell proteome analysis. Considering the high amount of biofilm biomass required for proteome analysis in parallel to undergoing investigations of the observed effect of AHD molecules, the analyses were performed at 128 µg/mL of saxagliptin and sitagliptin. Vildagliptin was exempted from the study due to its limited effect as observed by CLSM, whereas use of 2048 µg/mL of sitagliptin was not feasible owing to the high amounts of pure molecule required. Surprisingly, relatively few differentially expressed proteins were consistently detected.

Sitagliptin treatment and the *pepX* deletion both affected the expression of valine and proline amino acid tRNA-ligases, which may reflect perturbation of cytoplasmic amino acid pools and consequently an overall stress as observed under CLSM. The alteration of the level of cell surface antigen I/II (Okahashi et al., 1989) was of much interest, and this may correlate with the reduced hydrophobicity and biofilm formation exhibited by the mutant. The 12 proteins that were differentially expressed in response to both drug treatments were noted to include enolase (SMU.1247), which can be a moonlighting surface-associated protein in *S. mutans* (Ge et al., 2004), and acetate kinase (SMU.1978), which participates in the Pta-Ack pathway that can influence biofilm formation (Kim et al., 2015).

Conclusions

Through this work we were able to establish a potential role of *pepX* in biofilm development of *S.mutans* and moved a step forward in the identification and development of novel Sm-DPP IV inhibitors. We have also tried to demonstrate the likely effect of AHD drugs on bacteria, as a proof of the concept that many regularly used drugs may exert some sort of side activity against microbes transiently or permanently inhabiting the human body. Future studies are focused on searching or synthesizing molecules targeting Sm-DPP IV that may be applicable as a new anti-caries agent and studying the effect of drug molecules on *S. mutans* biofilms formed on hydroxylapatite discs and, ultimately, mixed species biofilms.

Acknowledgement

We acknowledge Prof. Giovanni Di Bonaventura and Prof. Simone Guarnieri at Università "G. d'Annunzio" Chieti-Pescara for their help in CLSM studies.

309 Funding: This work was supported by Ministero dell'Istruzione e della Ricerca Scientifica -
310 ITALY (grant PRIN project 2009 no. 2009P5EKH4_003 - to GL) and by the University of
311 Camerino (grant no. FPA00057 - to VLA).

312 **Conflicts of Interests**

313 The authors declare no conflicts of interest.

References

Ahn, S.J., Ahn, S.J., Wen, Z.T., Brady, L.J., Burne, R.A., 2008. Characteristics of biofilm formation by Streptococcus mutans in the presence of saliva. Infect. Immun. 76, 4259–68. doi:10.1128/IAI.00422-08

Ahn, S.J., Cho, E.J., Kim, H.J., Park, S.N., Lim, Y.K., Kook, J.K., 2012. The antimicrobial effects of deglycyrrhizinated licorice root extract on Streptococcus mutans UA159 in both planktonic and biofilm cultures. Anaerobe 18, 590–6. doi:10.1016/j.anaerobe.2012.10.005

Ajdić, D., McShan, W.M., McLaughlin, R.E., Savić, G., Chang, J., Carson, M.B., Primeaux, C., Tian, R., Kenton, S., Jia, H., Lin, S., Qian, Y., Li, S., Zhu, H., Najar, F., Lai, H., White, J., Roe, B. a, Ferretti, J.J., 2002. Genome sequence of Streptococcus mutans UA159, a cariogenic dental pathogen. Proc. Natl. Acad. Sci. U. S. A. 99, 14434–9. doi:10.1073/pnas.172501299

Bagramian, R.A., Garcia-Godoy, F., Volpe, A.R., 2009. The global increase in dental caries. A pending public health crisis. Am. J. Dent. 22, 3–8.

Boulos, L., Prevost, M., Barbeau, B., Coallier, J., Desjardins, R., 1999. Methods LIVE / DEAD ® Bac Light E : application of a new rapid staining method for direct enumeration of viable and total bacteria in drinking water 37, 77–86.

Boulton, D.W., Kasichayanula, S., Keung, C.F.A., Arnold, M.E., Christopher, L.J., Xu, X.S., Lacreta, F., 2013. Simultaneous oral therapeutic and intravenous ^{14}C-microdoses to determine the absolute oral bioavailability of saxagliptin and dapagliflozin. Br. J. Clin. Pharmacol. 75, 763–8. doi:10.1111/j.1365-2125.2012.04391.x

CLSI, 2011. Performance Standards for Antimicrobial Susceptibility Testing; Twenty First Informational Supplement. Clinical and Laboratory Standards Institute.

Cowman, R.A., Baron, S.S., 1993. Comparison of aminopeptidase activities in four strains of mutans group oral streptococci. Infect. Immun. 61, 182–6.

Cowman, R.A., Baron, S.S., 1997. Pathway for Uptake and Degradation of X-Prolyl Tripeptides in Streptococcus mutans VA-29R and Streptococcus sanguis ATCC 10556. J. Dent. Res. 76, 1477–1484. doi:10.1177/00220345970760081001

Cowman, R.A., Perrella, M.M., Fitzgerald, R.J., 1975. Caseinolytic and glyoprotein hydrolase activity of Streptococcus mutans. J. Dent. Res. 55, 391–9.

da Silva, B.R., de Freitas, V.A.A., Carneiro, V.A., Arruda, F.V.S., Lorenzón, E.N., de Aguiar, A.S.W., Cilli, E.M., Cavada, B.S., Teixeira, E.H., 2013. Antimicrobial activity of the synthetic peptide Lys-a1 against oral streptococci. Peptides 42, 78–83. doi:10.1016/j.peptides.2012.12.001

De, A., Lupidi, G., Petrelli, D., Vitali, L.A., 2016. Molecular cloning and biochemical

characterization of Xaa-Pro dipeptidyl-peptidase from Streptococcus mutans and its inhibition by anti-human DPP IV drugs. FEMS Microbiol. Lett. 363, fnw066. doi:10.1093/femsle/fnw066

Fred, A., 2009. Pharmacokinetis tabulated summary. [WWW Document]. NDA no. 22-350. URL http://www.accessdata.fda.gov/drugsatfda_docs/nda/2009/022350s000_PharmR_P3.pdf (accessed 2.9.15).

Ge, J., Catt, D.M., Gregory, R.L., 2004. Streptococcus mutans surface alpha-enolase binds salivary mucin MG2 and human plasminogen. Infect. Immun. 72, 6748–52. doi:10.1128/IAI.72.11.6748-6752.2004

Ge, J., Feng, Y., Ji, H., Zhang, H., Zheng, F., Wang, C., Yin, Z., Pan, X., Tang, J., 2009. Inactivation of dipeptidyl peptidase IV attenuates the virulence of Streptococcus suis serotype 2 that causes streptococcal toxic shock syndrome. Curr. Microbiol. 59, 248–55. doi:10.1007/s00284-009-9425-8

Goldstein, J.M., Banbula, A., Kordula, T., Mayo, J.A., 2001. Novel Extracellular x-Prolyl Dipeptidyl-Peptidase (DPP) from Streptococcus gordonii FSS2 : an Emerging Subfamily of Viridans Streptococcal x-Prolyl DPPs. Infect. Immun. 69, 5494–5501. doi:10.1128/IAI.69.9.5494

Green, B.D., Flatt, P.R., Bailey, C.J., 2006. Dipeptidyl peptidase IV (DPP IV) inhibitors: A newly emerging drug class for the treatment of type 2 diabetes. Diab. Vasc. Dis. Res. 3, 159–65. doi:10.3132/dvdr.2006.024

Idkaidek, N., Arafat, T., 2012. Saliva versus plasma pharmacokinetics: theory and application of a salivary excretion classification system. Mol. Pharm. 9, 2358–63. doi:10.1021/mp300250r

Kim, J.N., Ahn, S.-J., Burne, R.A., 2015. Genetics and Physiology of Acetate Metabolism by the Pta-Ack Pathway of Streptococcus mutans. Appl. Environ. Microbiol. 81, 5015–5025. doi:10.1128/AEM.01160-15

King, H., Aubert, R., Herman, W., 1998. Global burden of diabetes 1995–2025. Diabetes Care 21, 1414–1431. doi:10.2337/diacare.21.9.1414

Lau, P.C.., Sung, C.K., Lee, J.H., Morrison, D.A., Cvitkovitch, D.G., 2002. PCR ligation mutagenesis in transformable streptococci: application and efficiency. J. Microbiol. Methods 49, 193–205. doi:10.1016/S0167-7012(01)00369-4

Malke, H., Reichardt, W., Hartmann, M., Walter, F., 1981. Genetic study of plasmid-associated zonal resistance to lincomycin in Streptococcus pyogenes. Antimicrob. Agents Chemother. 19, 91–100. doi:10.1128/AAC.19.1.91

Nance, W.C., Dowd, S.E., Samarian, D., Chludzinski, J., Delli, J., Battista, J., Rickard, A.H., 2013. A high-throughput microfluidic dental plaque biofilm system to visualize and quantify the effect of antimicrobials. J. Antimicrob. Chemother. 68, 2550–60. doi:10.1093/jac/dkt211

388 Okahashi, N., Sasakawa, C., Yoshikawa, M., 1989. Molecular characterization of a surface
389 protein antigen gene from serotype c Streptococcus mutans, implicated in dental caries.
390 Mol. Microbiol. 3, 673–678. doi:10.1111/j.1365-2958.1989.tb00215.x

391 Petersen, F.C., Scheie, A.A., 2000. Genetic transformation in Streptococcus mutans requires a
392 peptide secretion-like apparatus. Oral Microbiol. Immunol. 15, 329–334.
393 doi:10.1034/j.1399-302x.2000.150511.x

394 Rosengren, L., Winblad, B., 1976. Proteolytic activity of Streptococcus mutans (GS-5). Oral
395 Surgery, Oral Med. Oral Pathol. 42, 801–809. doi:10.1016/0030-4220(76)90103-1

396 Selwitz, R.H., Ismail, A.I., Pitts, N.B., 2007. Dental caries. Lancet 369, 51–9.
397 doi:10.1016/S0140-6736(07)60031-2

398 Villhauer, E.B., Brinkman, J. a., Naderi, G.B., Burkey, B.F., Dunning, B.E., Prasad, K.,
399 Mangold, B.L., Russell, M.E., Hughes, T.E., 2003. 1-[[(3-Hydroxy-1-
400 adamantyl)amino]acetyl]-2-cyano-(S)-pyrrolidine: A potent, selective, and orally
401 bioavailable dipeptidyl peptidase IV inhibitor with antihyperglycemic properties. J. Med.
402 Chem. 46, 2774–89. doi:10.1021/jm0300911

403 Wang, A., Dorso, C., Kopcho, L., Locke, G., Langish, R., Harstad, E., Shipkova, P.,
404 Marcinkeviciene, J., Hamann, L., Kirby, M.S., 2012. Potency, selectivity and prolonged
405 binding of saxagliptin to DPP4: maintenance of DPP4 inhibition by saxagliptin in vitro and
406 ex vivo when compared to a rapidly-dissociating DPP4 inhibitor. BMC Pharmacol. 12, 2.
407 doi:10.1186/1471-2210-12-2

408 Yagishita, H., Kumagai, Y., Konishi, K., Takahashi, Y., Aoba, T., Yoshikawa, M., 2001.
409 Histopathological studies on virulence of dipeptidyl aminopeptidase IV (DPPIV) of
410 Porphyromonas gingivalis in a mouse abscess model: use of a DPPIV-deficient mutant.
411 Infect. Immun. 69, 7159–61. doi:10.1128/IAI.69.11.7159-7161.2001

412

Figure Legends

Fig.1.Quantification of biofilm formed by *S. mutans* in the presence of AHD drugs and of biofilm formed by a *pepX* deletion mutant. A. The histogram represents mean % biofilm formation in minimal medium containing 0-2048 µg/mL AHD drugs (n = 4, with duplicates within each independent experiment), B. Comparison of biofilm formation between Δ*pepX* (in black) and wild-type (in white) *S. mutans* in minimal medium containing glucose (n = 3, performed in triplicates within each independent experiment). Error bars represent standard deviation (p-value <0.001). Insert: viable cells count (expressed as CFU/mL) in the planktonic phase over the biofilm formed in SDM containing glucose.

Fig. 2. CLSM comparative study of biofilms formed by the Δ*pepX* mutant and wild-type *S. mutans* after 20 h. (a) Δ *pepX* mutant (1st field), (b) Δ *pepX* mutant (2nd field), (c) wildtype (1st field), (d) wild-type (2nd field), (e) z-axis representation of biofilm formed by Δ *pepX* mutant, (f) z-axis representation of biofilm formed by wild-type.

Fig. 3. CLSM images of *S. mutans* untreated controls and treated with AHD drugs. (a) Untreated (1st field), (b) Untreated (2nd field), (c) Untreated (3rd field), (d) 128µg/mL saxagliptin treated, (e) 512µg/mL saxagliptin treated (1st field), (f) 512µg/mL saxagliptin treated (2nd field), (g) 512µg/mL vildagliptin treated, (h) 2048µg/mL sitagliptin treated (1st field), (i) 2048µg/mL sitagliptin treated (2nd field).

Tables

Table 1. EC_{50} values for each drug. Mean concentration of drug producing 50% reduction in biofilm formation (EC_{50}) was calculated from four independent replicates. Standard deviations (SD) were also determined.

Drug	EC_{50}± SD (µg/mL)
Saxagliptin	**205 ± 71**
Vildagliptin	**280 ± 150**
Sitagliptin	**167 ± 67**

Table 2. **Oligonucleotide DNA primers used in the present study.**

Name	Forward (5' → 3')	Reverse (5' → 3')	Purpose
Ery-pOMZ291	TAATCCATGGCACAAGTGATTTGTGATTGTTG	TAATGAGCTCTAGGCGCTAGGGACCTCTTT	Erythromycin cassette amplification
pepX-Up	ATTGTCTTTTGCGTAGCATCTT	TAATGAGCTCAAACCGTTCGTGATAACAGC	5' fragment for *pepX* deletion
pepX-Dn	TAATCCATGGAGGTCGCTAAGTTTGCTTTATTG	TCCACAGCTGAGATAGTAGAGAATG	3' fragment for *pepX* deletion

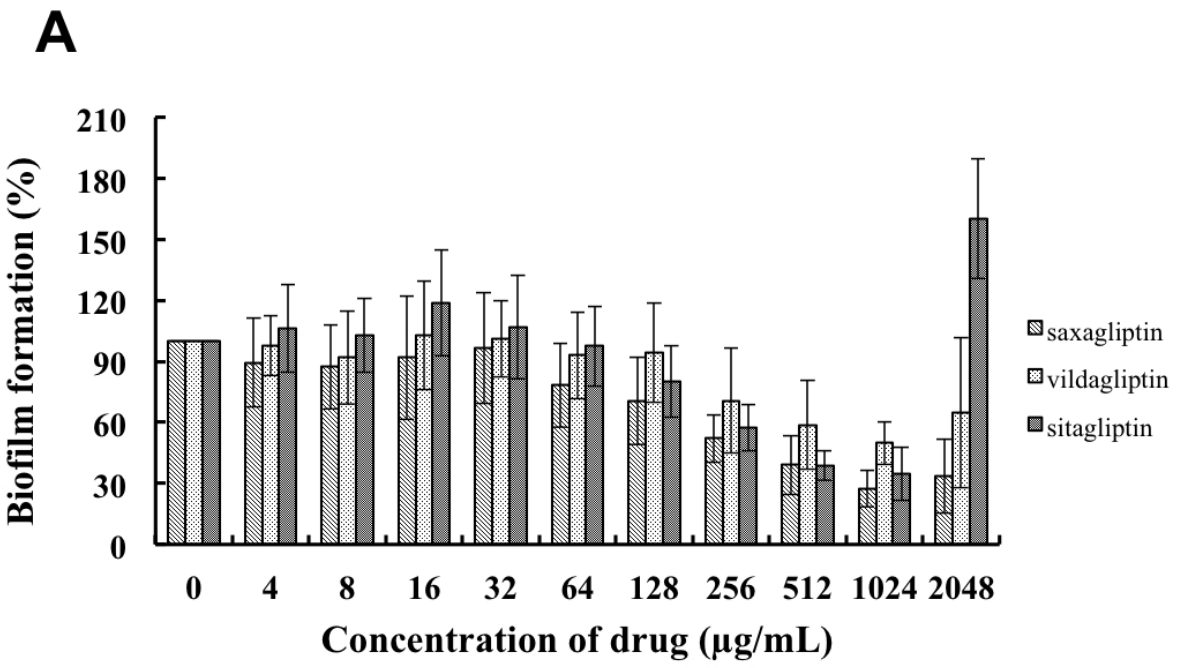
A
Biofilm formation (%)
210
180
150
120
90
60
30
0
0
4
8
16
32
64
128
256
512
1024
2048
Concentration of drug (μg/mL)
saxagliptin
vildagliptin
sitagliptin

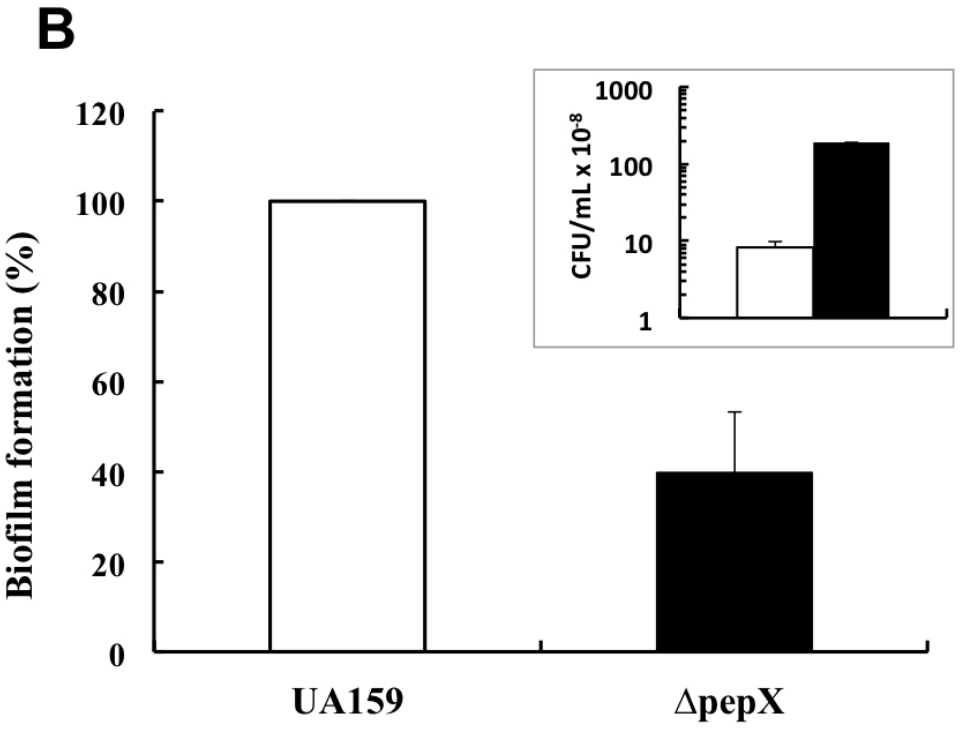
B
Biofilm formation (%)
120
100
80
60
40
20
0
UA159
ΔpepX
CFU/mL x 10-8
1000
100
10
1

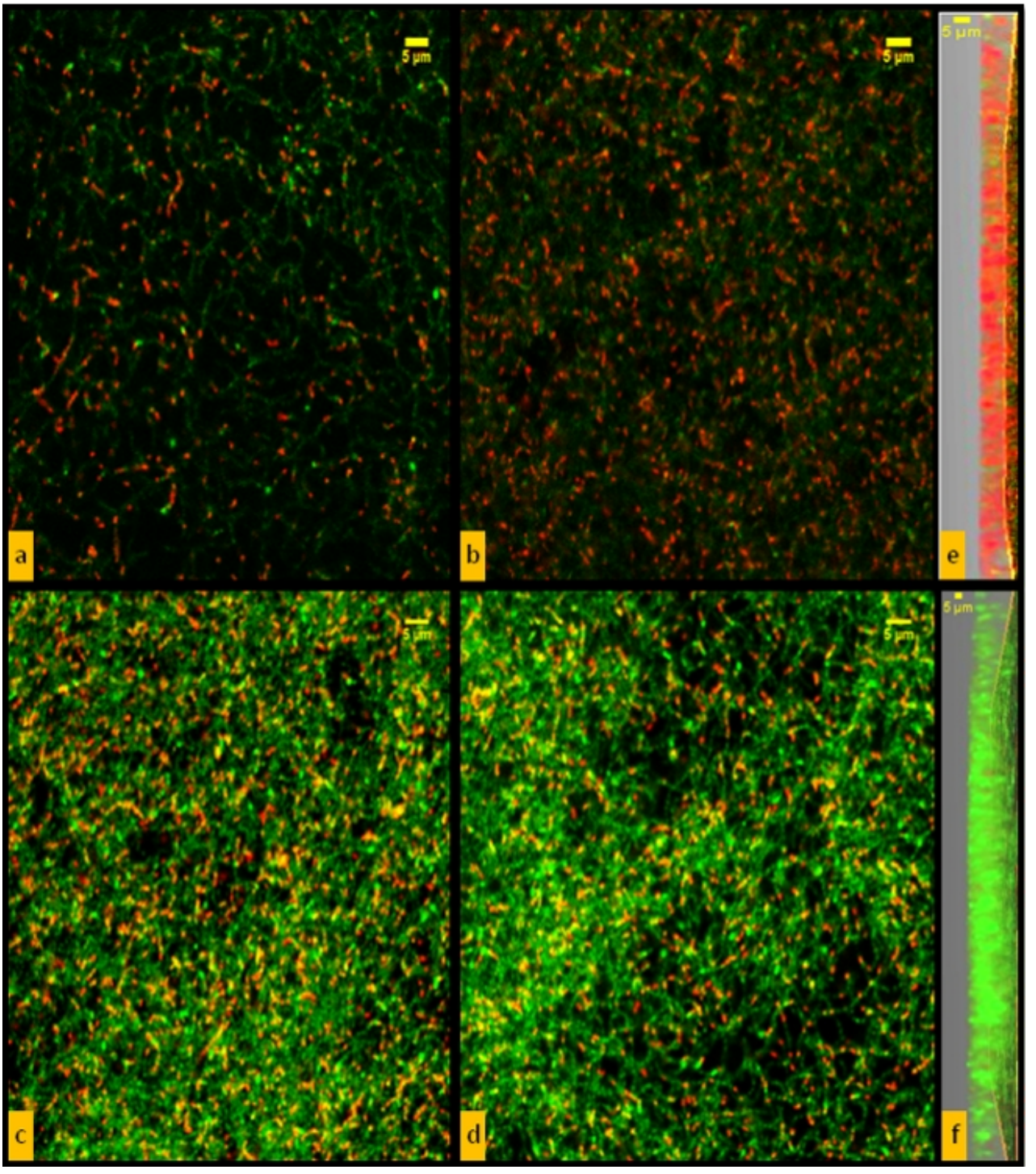
5 µm
a
5 µm
b
5 µm
e
5 µm
c
5 µm
d
5 µm
f

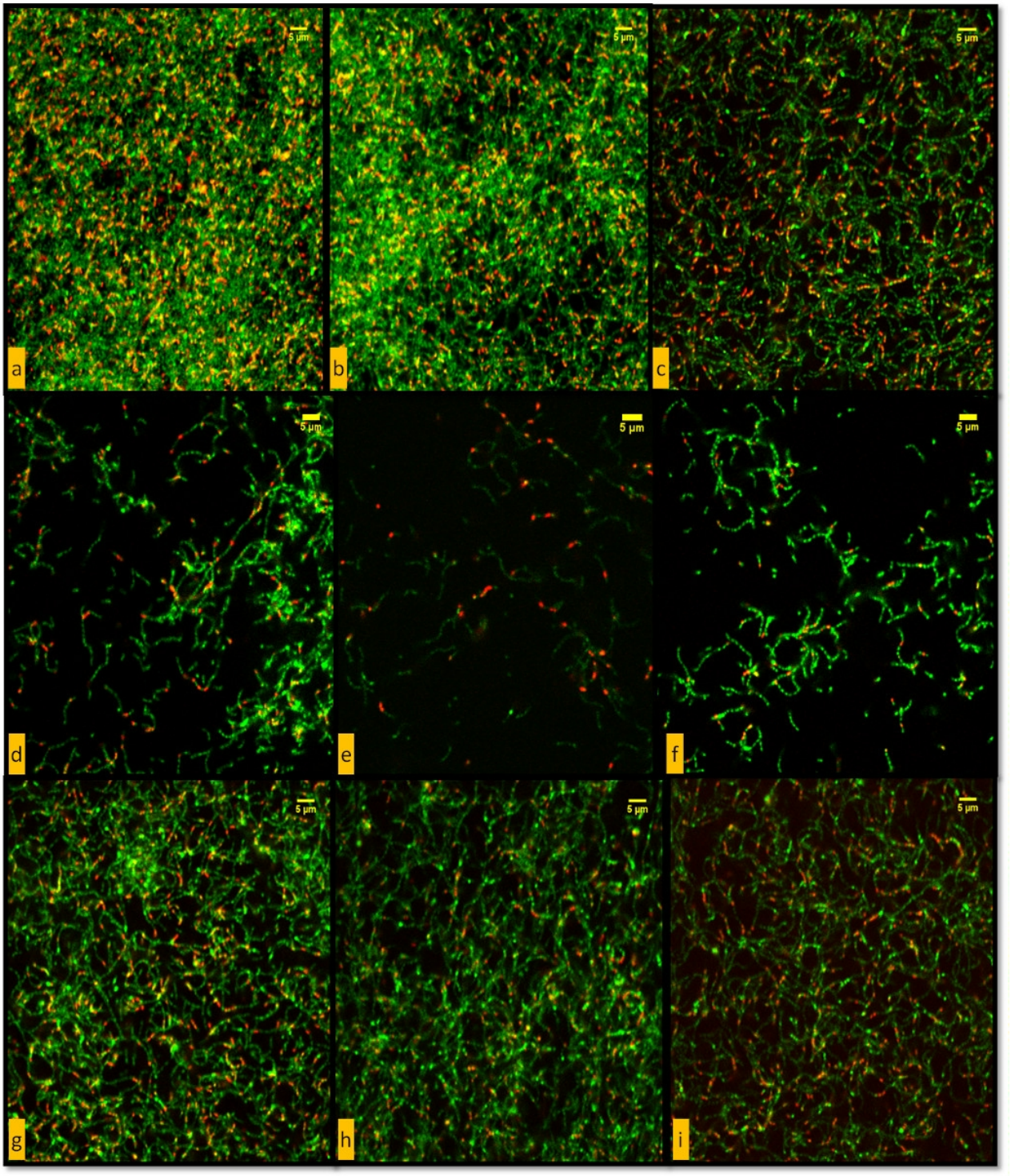
a
5 µm
b
5 µm
c
5 µm
d
5 µm
e
5 µm
f
5 µm
g
5 µm
h
5 µm
i
5 µm

Supplementary information

Title

Antidiabetic "gliptins" affect biofilm formation by *Streptococcus mutans*

Authors

Arpan De[1], Arianna Pompilio[2,3], Jenifer Francis[4], Iain Sutcliffe[4], Gary Black[4], Giulio Lupidi[1], Dezemona Petrelli[5], Luca A. Vitali[1]*

Authors' affiliation

1. School of Pharmacy, University of Camerino, Camerino, Italy.
2. Department of Medical, Oral and Biotecnological Sciences, School of Medicine, "G. d'Annunzio" University of Chieti-Pescara
3. Center of Excellence on Ageing, "G. d'Annunzio" University Foundation, Chieti.
4. Department of Applied Sciences, Faculty of Health & Life Sciences, Northumbria University, Newcastle upon Tyne, UK
5. School of Biosciences and Veterinary Medicine, University of Camerino, Camerino, Italy.

Fig.S1. Scatter plot of effect of each AHD molecule representing data points of four independent experiments (performed in duplicates within). Each data point corresponds to mean of the absorbance values (n = 2) at 495nm, at each concentration of AHD molecule while the data point at control or 0 µg/mL represents mean of absorbance values (n = 3) at the same wavelength. The absorbance values at 495 nm quantify the amount of extracted crystal violet by ethanol, in each biofilm assay. a. absorbance values at each concentration of saxagliptin, b. absorbance values at each concentration of vildagliptin, c. absorbance at each concentration of sitagliptin.

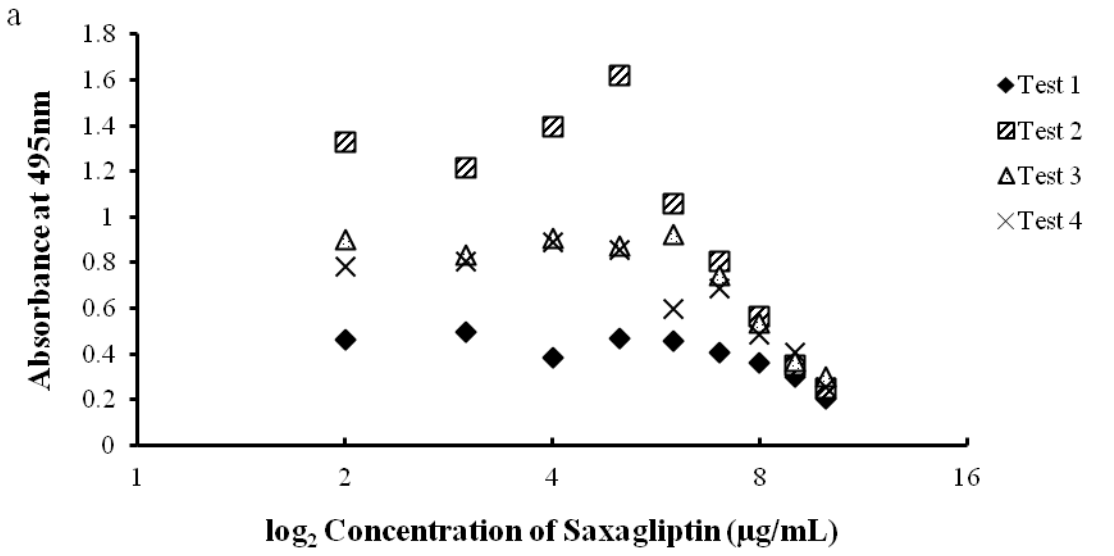

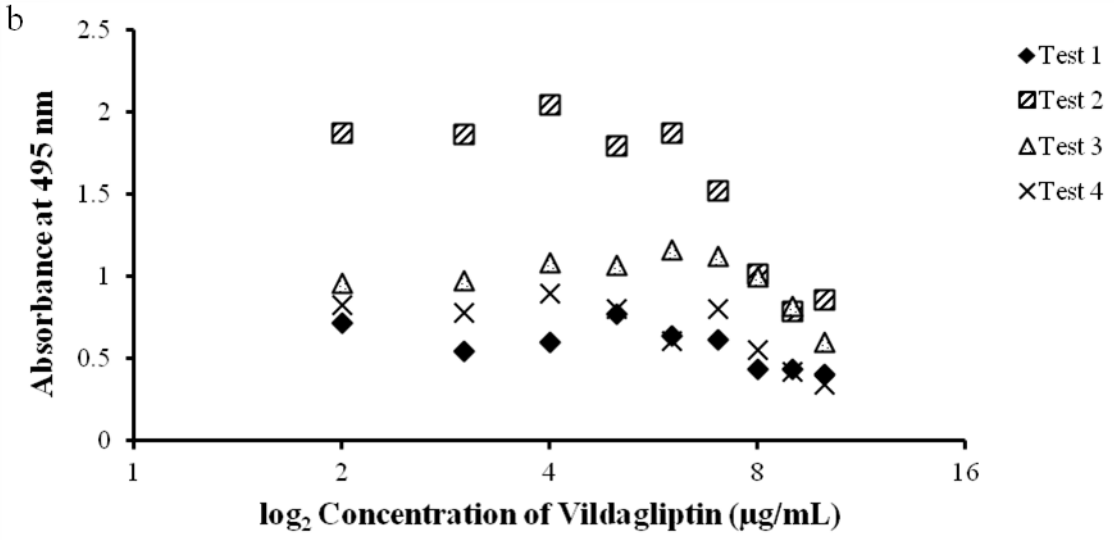

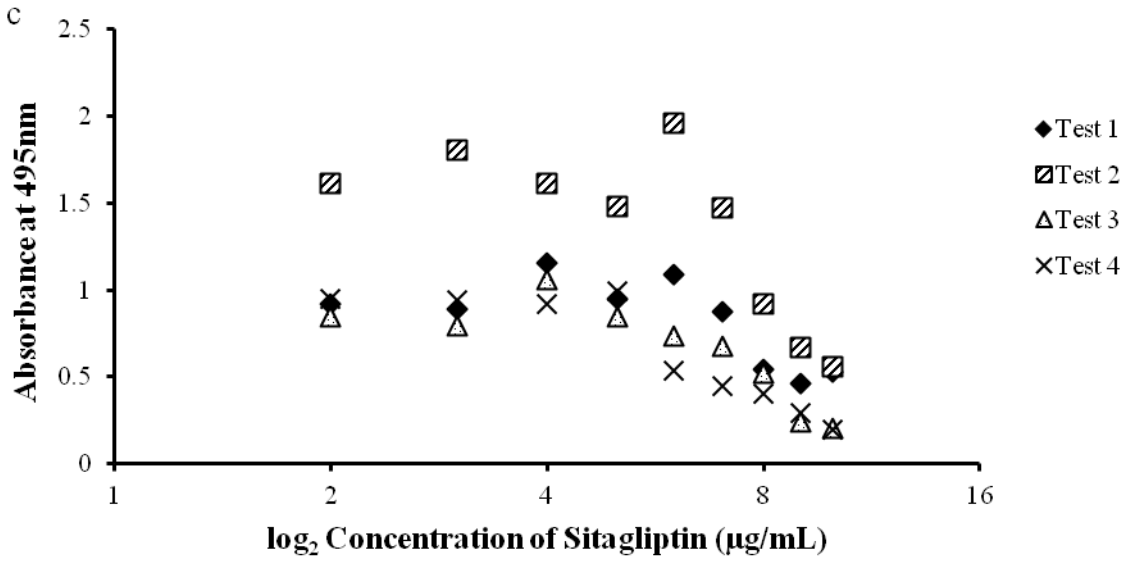

Fig.S2. Plots showing the pairwise estimated difference between means of the biofilm formed at two different concentrations of (a) Saxagliptin and (b) Sitagliptin. Statistical test was performed by multiple comparisons (all possible pairs of means) and Fisher's least significant difference (LSD) procedure. Pairs for which one mean was significantly different from the other (95% confidence level) were in red when positive and in cyan when negative.

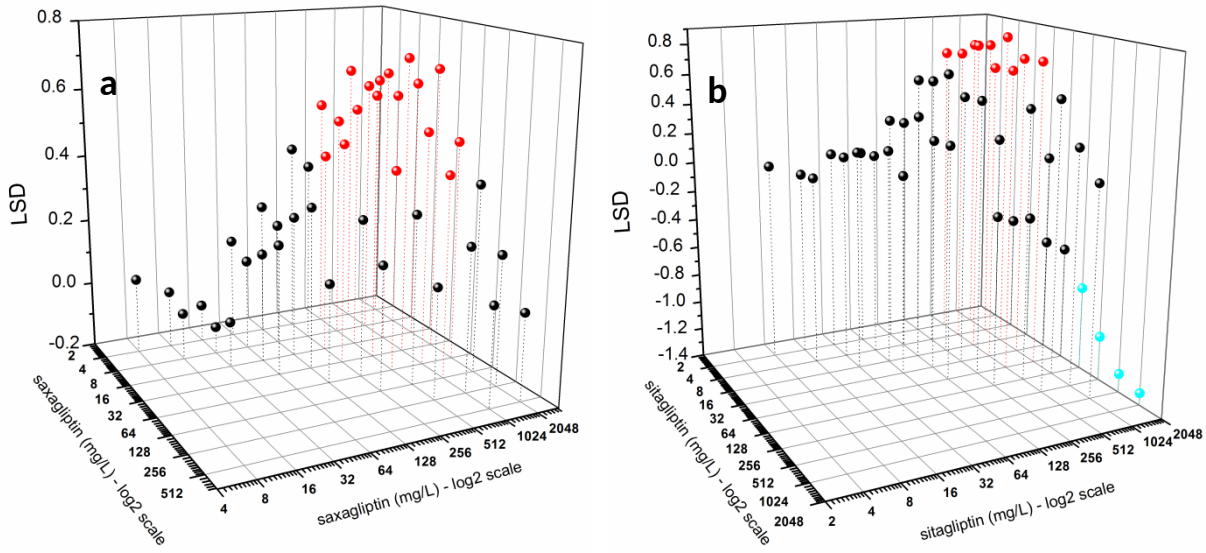

Fig. S3. Determination of cell viability of the planktonic phase in a biofilm assay at each concentration of AHD molecule. The platings were done in triplicates on BHI agar and mean of CFU/mL is reported as (–) in the scatter plot. Sitagliptin (●), Saxagliptin (■), Vildagliptin (▲).

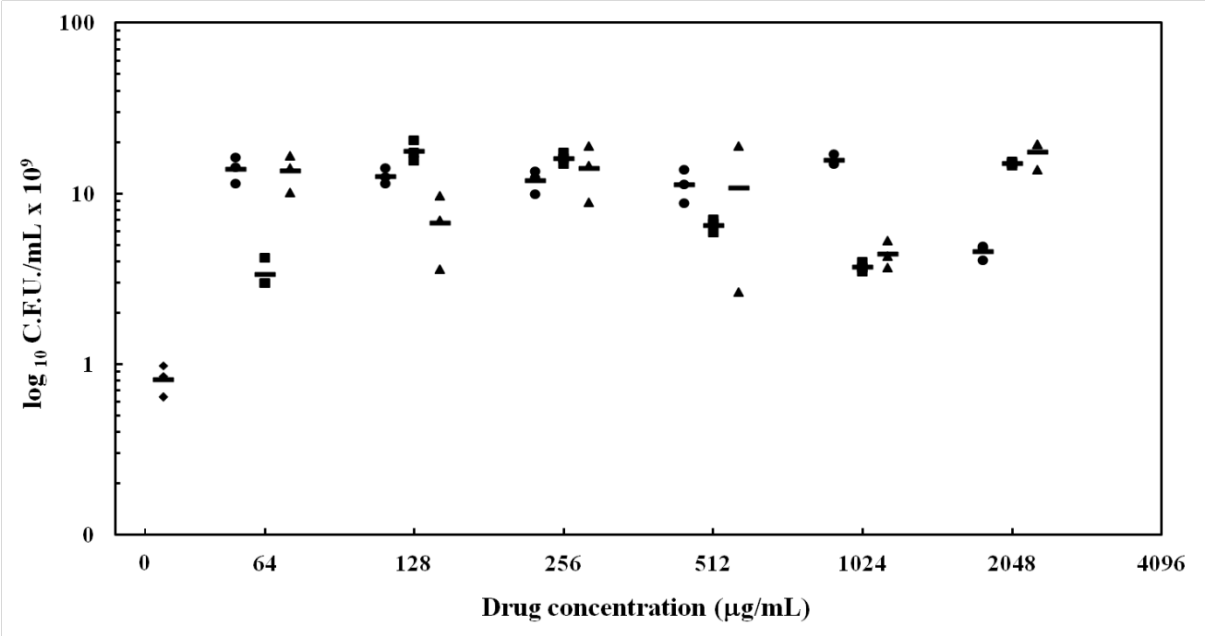

Fig. S4. Growth curves in SDM + glucose until 24 hrs incubation time. Circles: Colony Forming Units/mL (CFU/mL); Triangles: Optical Density units at 600 nm/mL (OD_{600}/mL). Filled: wildtype (*S. mutans* UA159); Open: Δ*pep*X mutant.

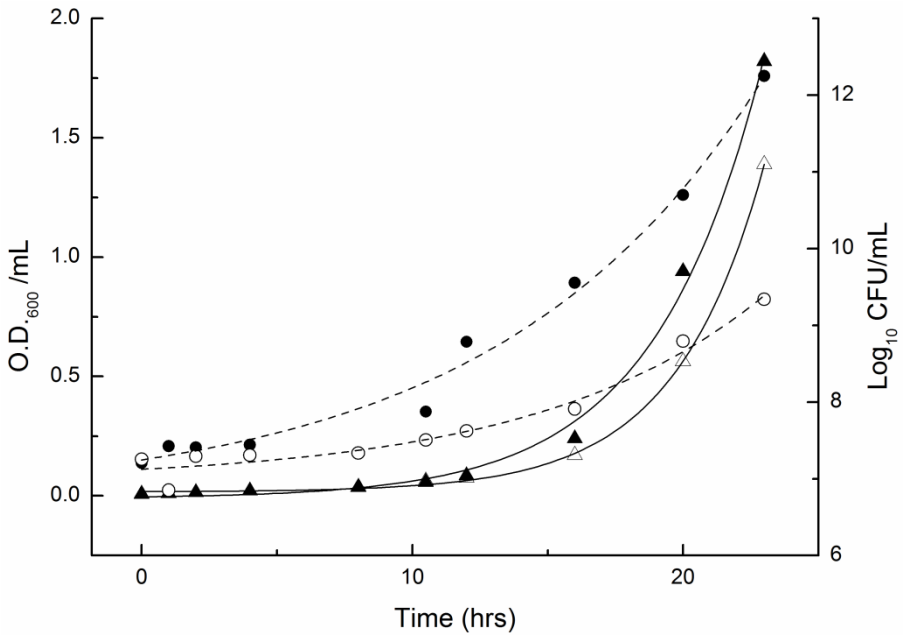

Fig. S5. Images and biofilm forming assay using crystal violet semiquantitative method at higher concentrations of sitagliptin. A sudden upsurge of biofilm formation at 2048 µg/mL of sitagliptin is represented as images. A. before washing of unattached cells, B. after three washes of unbound cells using saline, and C. after crystal violet staining and two subsequent washes.

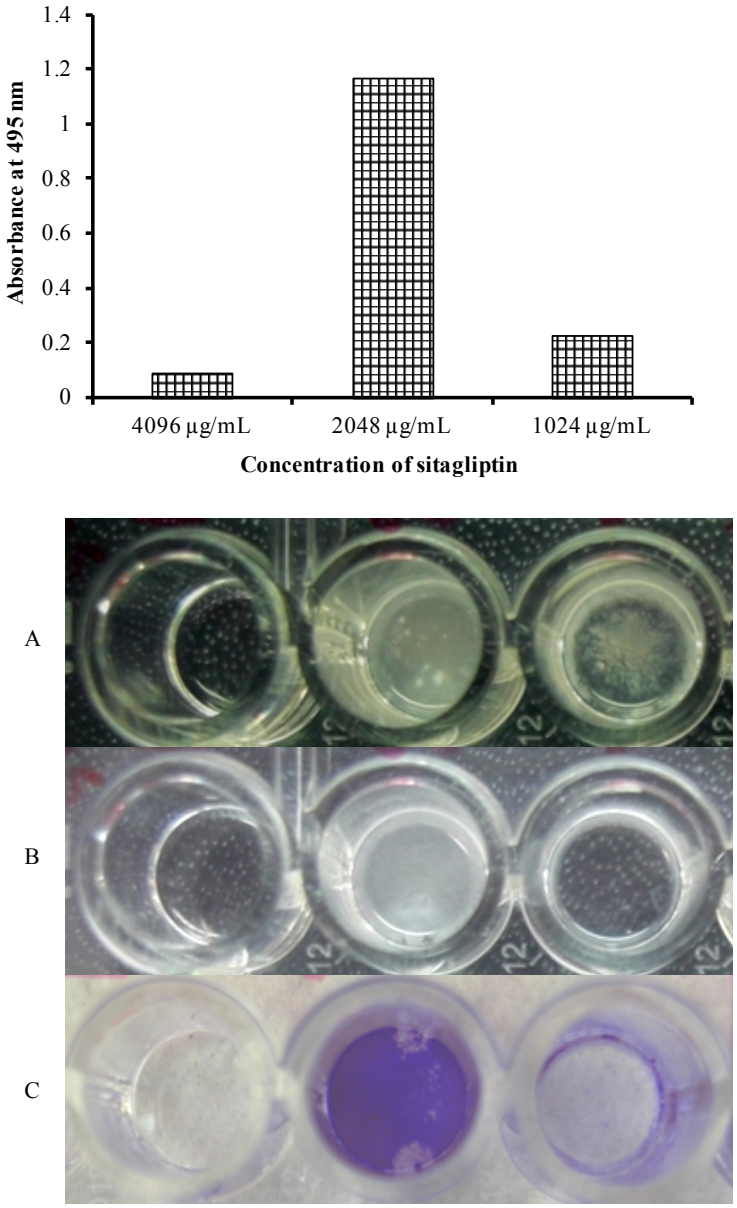

Supplementary Texts

Text 1. Preparation of Semi-Defined biofilm medium (SDM)

Semi-Defined biofilm medium either in 20mM glucose or sucrose contained 58mM K2HPO4, 15mM KH2PO4, 10mM (NH4)2SO4, 35mM NaCl, 0.2% Casamino acids and filter sterilized 40µM Nicotinic acid, 100µM Pyrridoxine HCl, 10µM Pantothenic acid, 1µM Riboflavin, 0.3µM Thiamine HCl, 0.05µM D-Biotin, 4mM L-Glutamic acid, 1mM L-Arginine HCl, 1.3mM L-Cysteine HCl, 0.1mM L-Tryptophan, 2mM MgSO4.7H2O. While preparation, salts and glucose or sucrose were autoclaved separately, whereas filter sterilized amino acids and vitamins were added in the medium at room temperature.

Text 2. Proteome analysis of biofilm grown cells

Protein isolation and pre-fractionation

The proteome of biofilm grown cells, either in absence or presence of an AHD drug, and that of the Δ*pepX* mutant were analysed from 48mL of culture. The biofilm for each condition was set up in a 24 well cell culture plate (Greiner Bio-one, CELLSTAR) as described above. After 20 hours of incubation the planktonic phase was removed and the attached biofilm was disrupted using sterile water. The harvested cells were pooled and washed twice in PBS (1X), resuspended in lysis buffer and sonicated at 12000 – 13000 microns amplitude for 2 minutes with an intermittent 10 sec on and 10 sec off in ice. Subsequently, the cell free extract was collected by centrifugation at 14000 × g for 45 min at 4°C and acetone precipitated at -20°C overnight. The precipitated proteins were collected by centrifugation, washed in 80% and 40% acetone successively, air dried for 1 hour at room temperature and stored at -20°C for further use. The pellet was dissolved in 30mM Tris buffer (pH 8) and then partially pre-fractionated by 1D PAGE. A similar amount of calculated protein (µg) as estimated by

Bradford assay, representing samples at each condition, was boiled with 5µL of loading dye for 15 min and electrophoresed at 200V for about 1 hr. The gel was stained in Coomassie Blue for 15 min followed by destaining overnight at room temperature.

Sample preparation and Mass spectrometry

The protein containing gel was sectioned into pieces and then treated twice with 100mM NH_4HCO_3 and acetonitrile (ACN) with shaking for 30 min allowing removal of the Coomassie stain. The gel slices were then dehydrated in ACN at room temperature for 60 min, air dried for 15 min and pre-incubated in 40µg/mL trypsin (Trypsin Gold, MS Grade, Promega) at 37°C for 1 hour in a water-bath. Subsequently, the gel pieces were immersed in NH_4HCO_3 and incubated further at 37°C overnight. On the following day, the digestion was stopped by adding 50% ACN (v/v) and 5% formic acid (v/v) with shaking for 30 min. The digested extract containing peptides was removed and transferred into a fresh vial (Fraction A). The gel pieces were further extracted using 83% ACN (v/v) and 0.2% formic acid under the same conditions (Fraction B). All the extracts containing digested peptides were then pooled (Fraction A + Fraction B) and frozen at -80°C for more than an hour. Frozen peptide digests were freeze-dried for 20- 24 hours (Alpha 1-2 LoPlus CHRIST attached to JAVAC High Vacuum pump). The samples were stored at -80°C until injection into the LC-MS/MS. Before injection, the lyophilized peptide digest was mixed in 5% ACN and 0.1% formic acid (v/v) and then run in a LC- NanoPump coupled to a tandem mass spectrometer (Thermo Q Exactive attached to HPLC Ultimate 3000 RSLC nano system), through an Easy Spray C18 column (PepMap RSLC, 75µm × 500mm, Thermo Scientific) equipped with Electro Spray Ionization, in a gradient solvent mixture of water and ACN containing 0.1% formic acid. The run was carried out for 215 minutes at a flow rate of 0.3µL/min with a scan range of 350 – 1800 m/z.

Identification of the peptides

The mass spectrum data (MS and MS2) obtained for each set of conditions was then processed in Progenesis LC-MS v4.1. The statistically validated peptides (>2 fold change in expression and features significantly present in all of the three technical replicates, $p < 0.05$) were exported into MASCOT database for identification (Matrix Science, www.matrix-science.com). The database search was performed for MS/MS spectra of all selected peptides with carbamidomethyl and oxidised methionine as modifications, and peptide mass tolerance of ±20 ppm. After identification, peptides were imported back into Progenesis for refining for only those protein matches from S. mutans, reviewing and removing all the proteins with conflict, grouping all the peptides with similar protein labels, quantifying abundance level of proteins and producing a compiled report on the differential level of proteins at different conditions. To ensure robust protein identification, only those proteins consistently detected in both biological replicates, typically with a minimum of >1 peptide per protein in each run, were retained for further analysis.

Supplementary Tables

Table S1. Differentially expressed protein identified by proteomic analysis of *S. mutans* biofilms (** these protein were only identified on the basis of 1 peptide in one of the biological replicates).

More abundant in SAXAGLIPTIN control cells		
Protein id.	**Protein name/annotation**	**Expression ratio n=2**
SMU.446	Glycine--tRNA ligase beta subunit	1.8
SMU.910	Glucosyltransferase-S	2.1
SMU.1004	Glucosyltransferase-I	2.1
SMU.1005	Glucosyltransferase-SI	2.5
SMU.2028	Levansucrase (ftf)	2.2
SMU.2031	Elongation factor Ts	2.1
More abundant in SAXAGLIPTIN treated cells		
Protein id.	**Protein name/annotation**	**Expression ratio n=2**
SMU.23	Ribose-phosphate pyrophosphokinase 1	1.6
SMU.34	Phosphoribosylformylglycinamidine cyclo-ligase	1.8
SMU.359	Elongation factor G	2.0
SMU.361	Phosphoglycerate kinase	2.1
SMU.402	Formate acetyltransferase (pfl)	2.6
SMU.421	Translation initiation factor IF-2**	2.1
SMU.471	Cell cycle protein GpsB	1.8
SMU.558	Isoleucine--tRNA ligase	3.6
SMU.676	NADP-dependent glyceraldehyde-3-phosphate dehydrogenase	1.7
SMU.712	Phosphoenolpyruvate carboxylase**	2.7
SMU.714	Elongation factor Tu	2.4

SMU.860	Carbamoyl-phosphate synthase large chain**	2.6
SMU.1060	Signal recognition particle protein	2.3
SMU.1066	GMP synthase [glutamine-hydrolyzing]	2.0
SMU.1115	L-lactate dehydrogenase	2.0
SMU.1247	Enolase	1.9
SMU.1656	Phosphoserine aminotransferase	2.1
SMU.1673	Uracil phosphoribosyltransferase	2.5
SMU.1838	Protein translocase subunit SecA	1.8
SMU.1954	60 kDa chaperonin (groEL)	1.8
SMU.1978	Acetate kinase**	2.6
SMU.2101	Aspartate--tRNA ligase 2	2.1
SMU.2135c	30S ribosomal protein S4	7.5

More abundant in SITAGLIPTIN control cells		
Protein id.	**Protein name/annotation**	**Expression ratio n=2**
SMU.307	Glucose-6-phosphate isomerase	1.86
SMU.1457	dTDP-glucose 4,6-dehydratase	2.6
SMU.1770	Valine-tRNA ligase	28.0
SMU.1783	Proline-tRNA ligase	2.5
SMU.1786	Isoprenyl transferase	3.8
SMU.2031	Elongation factor Ts	1.6
More abundant in SITAGLIPTIN treated cells		
Protein id.	**Protein name/annotation**	**Expression ratio n=2**
SMU.23	Ribose-phosphate pyrophosphokinase 1	4.3

SMU.82	Chaperone protein DnaK	3.3
SMU.155	Polyribonucleotide nucleotidyltransferase	5.3
SMU.359	Elongation factor G	2.0
SMU.402	Formate acetyltransferase (pfl)	2.19
SMU.421	Translation initiation factor IF-2	3.6
SMU.712	Phosphoenolpyruvate carboxylase	1.8
SMU.714	Elongation factor Tu	3.0
SMU.856	Bifunctional protein PyrR	2.6
SMU.860	Carbamoyl-phosphate synthase large chain	1.7
SMU.900	4-hydroxy-tetrahydrodipicolinate reductase	2.4
SMU.910	Glucosyltransferase-S	2.9
SMU.1005	Glucosyltransferase-SI	9.0
SMU.1085	Peptide chain release factor 1	32.1
SMU.1247	Enolase	4.5
SMU.1467	Adenine phosphoribosyltransferase	16.4
SMU.1538	Glucose-1-phosphate adenylyltransferase	6.3
SMU.1635	Bifunctional protein GlmU	1.9
SMU.1673	Uracil phosphoribosyltransferase	4.0
SMU.1820c	Glutamyl-tRNA(Gln) amidotransferase subunit A	∞
SMU.1954	60 kDa chaperonin	34.4
SMU.1978	Acetate kinase**	3.1
SMU.1990	DNA-directed RNA polymerase subunit beta	3.5
SMU.1992	Tyrosine--tRNA ligase	9.1
SMU.2032	30S ribosomal protein S2	1.8
SMU.2128	Dihydroxy-acid dehydratase	2.3

More abundant in wild type compared to *pepX* mutant		
Protein id.	**Protein name/annotation**	**Expression ratio n=2**
SMU.82	Chaperone protein DnaK	2.2
SMU.610	Cell surface antigen I/II (spaP)	1.8
SMU.675	Phosphoenolpyruvate-protein phosphotransferase (ptsI)	1.8
SMU.1073	Formate-tetrahydrofolate ligase (fhs)	1.7
SMU.1770	Valine-tRNA ligase**	3.4
SMU.1783	Proline-tRNA ligase**	1.8
SMU.1838	Protein translocase subunit SecA	2.0
SMU.2008	50S ribosomal protein L30	2.5
SMU.2098	Arginine-tRNA ligase	2.5